

Precise Thickness Measurement in Si and SiO<sub>2</sub>  
by Electron Holography and Electron  
Energy-Loss Spectroscopy(電子線ホログラフィー  
と電子エネルギー損失分光法によるSiとSiO<sub>2</sub>の厚さ  
の精密測定)

著者	李昌祐
号	1998
発行年	2001
URL	<a href="http://hdl.handle.net/10097/10805">http://hdl.handle.net/10097/10805</a>

氏名	イ チャン ウ 李 昌 祐
授与学位	博士 (工学)
学位授与年月日	平成 13 年 10 月 10 日
学位授与の根拠法規	学位規則第 4 条第 2 項
最終学歴	1994 年 9 月 高麗大学大学院金属工学科物理金属専攻修士課程 修了
学位論文題目	Precise Thickness Measurement in Si and SiO <sub>2</sub> by Electron Holography and Electron Energy-Loss Spectroscopy (電子線ホログラフィーと電子エネルギー損失分光法による Si と SiO <sub>2</sub> の厚さの精密測定)
論文審査委員	主査 東北大学教授 進藤 大輔 東北大学教授 平賀 賢二 東北大学教授 我妻 和明

## 論 文 内 容 要 旨

### Chapter 1. Introduction

The precise measurement of sample thickness is very important for material analysis because the information of sample thickness makes quantitative analysis possible. From the quantitative analysis, we can predict the material properties such as mechanical and electrical property. For example, since precipitates like the phase of  $\eta'$  in aluminum alloy or dispersoids such as carbide in magnesium alloy disturb the dislocation moving, the density of precipitate and dispersoid is related to their strength, which is the main property on these materials. Another case, the density of dislocation, which exists in semiconductor, influences their electrical property, namely electron mobility and lifetime of carriers. So a number of workers have investigated energy levels associated with dislocation in deformed silicon. The thickness is also an essential parameter in correcting for the absorption and fluorescence of characteristic X-ray.

Although there are several methods available for thickness measurement with a transmission electron microscope (TEM), such as the convergent beam electron diffraction (CBED) method and the contamination method, each has its own limitation in accuracy and applicability. For example, the CBED method is only applicable to a specimen with good crystallinity, and the contamination method generally has a low accuracy.

Electron energy-loss spectrometer (EELS) and electron holography were developed as new techniques of thickness measurement. Comparing with the existing methods, they have some advantage on the thickness measurement such as application to not only a crystalline but also an amorphous materials and measurement of ultra-fine area. To measure thickness, however, mean free path ( $\lambda_p$ ) and mean inner potential ( $U_0$ ) is required for using EELS and electron holography. In this paper, accuracy of EELS and electron holography and the influence factors on thickness measurement by these methods were investigated by using an amorphous SiO<sub>2</sub> and a crystalline Si.

### Chapter 2. Experimental techniques

Electron holograms were collected with a JEM-3000F TEM, which is equipped with a field-emission gun (FEG) and a biprism, being operated at 300 kV. The voltage of the biprism was changed from 20V to 30V for

measurement of visibility. For estimate of mean inner potentials of Si and SiO<sub>2</sub>, the voltage of the biprism was set to be 40 V and 30 V. The holograms were recorded in films at 150K magnifications and enlarged to 8 times after digitizing the data through the film scanner (Nikon ; LS-3510AF).

Electron energy-loss spectra were measured by a JEM-3000F TEM equipped with a Gatan PEELS system (model 676) and a JEM-2010EF TEM attached with a  $\Omega$ -type energy filtering system being operated at 100 , 200 and 300 kV, respectively.  $\lambda_p$  was measured with collection angles between 1.6 and 23.4 mrad, under the condition of no objective aperture (157 mrad) at accelerating voltage of 200 kV. The intensity of electron energy-loss spectra was precisely measured using the imaging plate system (FDL-UR-V)

### Chapter 3. Measurement of visibility and charging on SiO<sub>2</sub> particle

The effects of biprism voltage and illumination angle on visibility and spacing of interference fringe were estimated and discussed. The visibility of interference fringes is estimated to be between 0.5 and 0.02 under the condition that biprism voltage has values between 20 – 90V as shown in Fig. 1. It is found that increase of biprism voltage leads to decrease the visibility of interference fringes. Also, in order to obtain good fringe visibility, larger illumination angle i.e., enough wide beam is necessary to take a hologram.

Also, the electric charge in amorphous SiO<sub>2</sub> particle is evaluated quantitatively. Figure 2 shows a hologram of a SiO<sub>2</sub> particle on the carbon grid (a), diffractogram (b) and reconstruction image, which phase is amplified by 10 times. Under the condition of no objective aperture and current density at 5.0 pA/cm<sup>2</sup>, amount of charging on SiO<sub>2</sub> particles are estimated to be  $9.94 \times 10^{-17}$  C and this charge is equal to the net loss of about 620 electrons emitted from SiO<sub>2</sub> particle since the elementary electric charge is  $1.6 \times 10^{-19}$  C. Regardless of the change of an incident electron intensity in the range of 0.3 – 5.0 pA/cm<sup>2</sup>, the amount of the electric charge in a SiO<sub>2</sub> particle decreases by 30 ~ 40 % with inserting objective aperture and this decrease of electric charging is possible to be neutralized by secondary electrons and back scattering electrons generated from objective aperture. The amount of the electric charge in a SiO<sub>2</sub> particle increases with the increase of incident electron intensity for both conditions of with and without an objective aperture.

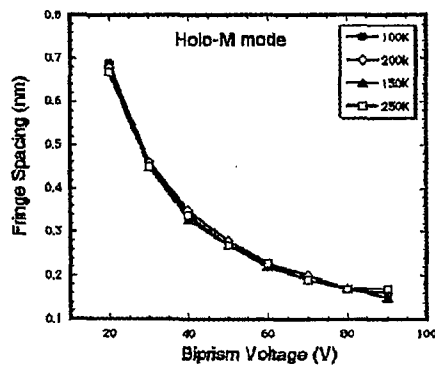


Fig.1. Dependence of interference fringe visibility on biprism voltage for JEM-3000F at 300 kV.

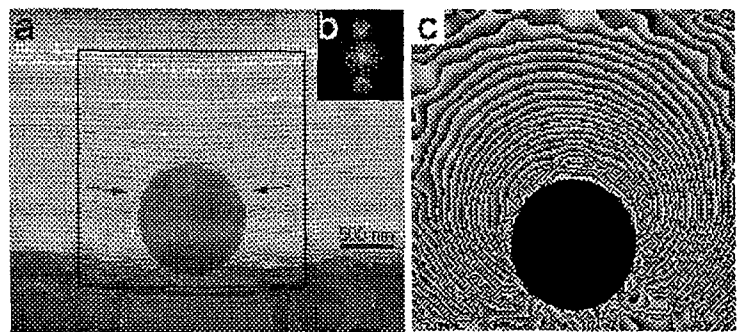


Fig.2. (a) Electron hologram of amorphous SiO<sub>2</sub> on the carbon microgrid. (b) FFT of the rectangular part in (a). (c) 10-times phase-amplified contour map on the rectangular part in (a)

### Chapter 4. Thickness measurement of amorphous SiO<sub>2</sub> by electron holography and EELS

Through the estimation of mean free path ( $\lambda_p$ ) for inelastic scattered electron and mean inner potential ( $U_0$ ) of

an amorphous SiO<sub>2</sub>, accuracy of thickness measurement by EELS and electron holography on amorphous SiO<sub>2</sub> particles is estimated and discussed. From EELS, the mean free path ( $\lambda_p$ ) of an amorphous SiO<sub>2</sub> was estimated to be  $178 \pm 4$  nm under the condition of no objective aperture at 200 kV. Under no objective aperture condition, which means that collection angle is 157 mrad,  $\lambda_p$  for inelastic scattered electron of amorphous SiO<sub>2</sub> was found to decrease with the decreasing of accelerating voltage (i.e.,  $\lambda_p = 100 \pm 2$  nm at 100 kV,  $\lambda_p = 178 \pm 4$  nm at 200 kV and  $\lambda_p = 247 \pm 4$  nm at 300 kV) as shown in Fig. 3 (a). On the effect of collection angle on  $\lambda_p$ , it is found that  $\lambda_p$  increases rapidly with the decreasing of collection angles from 18.5 mrad to 1.6 mrad, whereas there are no changes above 18.5 mrad at 200 kV as shown in Fig. 3 (b). Considering the theoretical background, the minimum thickness that could be measured using EELS at 300 kV was found to be about 30 nm for amorphous SiO<sub>2</sub>.

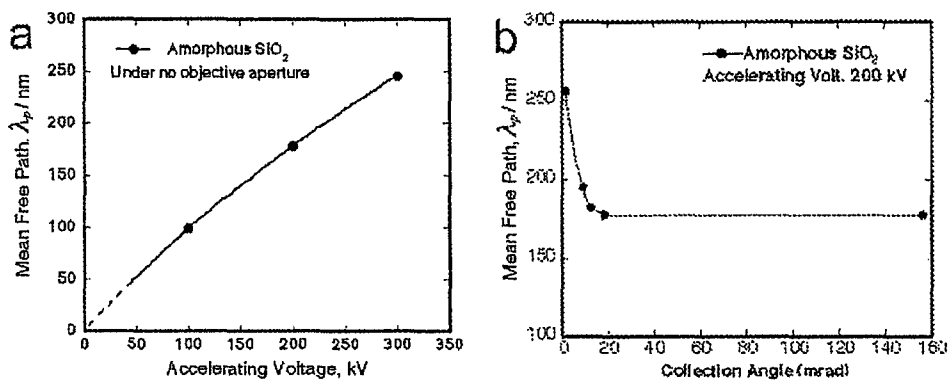


Fig. 3 The effect of accelerating voltage (a) and collection angle (b) on the mean free path of amorphous SiO<sub>2</sub>.

Figure 4 shows a hologram of a part of amorphous SiO<sub>2</sub> particle. As indicated by arrows in Fig. 4, the phase shift of the interference fringes was clearly observed around the particle surface. From the hologram, the mean inner potential ( $U_0$ ) of amorphous SiO<sub>2</sub> was evaluated to be  $11.5 \pm 0.3$  V. If it is considered that the accuracy in the analysis of holograms was evaluated to be  $\pm 0.06\pi$ , the minimum thickness that could be measured using electron holography at 300 kV was found to be less than 6 nm for amorphous SiO<sub>2</sub>. The accurate thickness measurement in a thinner region is more possible for electron holography than EELS in amorphous SiO<sub>2</sub>.

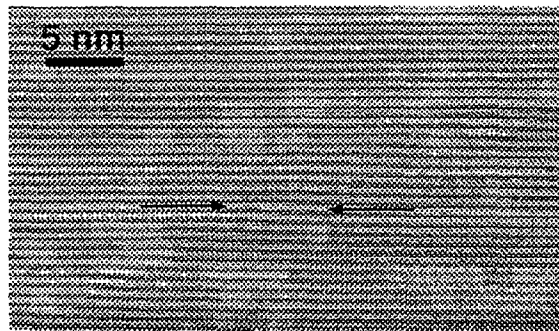


Fig. 4 A hologram of a part of SiO<sub>2</sub> particle.

## Chapter 5 Thickness measurement of single crystal Si by electron holography and EELS

For crystalline Si, mean free path ( $\lambda_p$ ) and mean inner potential ( $U_0$ ) of a crystalline Si are estimated and the accuracy of electron holography and EELS on thickness measurement is discussed. The mean free path ( $\lambda_p$ ) of a crystalline Si was estimated to be  $147 \pm 5$  nm under the condition of no objective aperture at 200 kV by using EELS. Under no objective aperture condition (collection angle is 157 mrad),  $\lambda_p$  for inelastic scattered electron of a crystalline Si was found to decrease with the decreasing of accelerating voltage (i.e.,  $\lambda_p = 97 \pm 3$  nm at 100 kV,  $\lambda_p = 147 \pm 5$  nm at 200 kV and  $\lambda_p = 180 \pm 6$  nm at 300 kV).  $\lambda_p$  increases rapidly with the decreasing of

collection angles from 2.1 mrad to 23.4 mrad, whereas there is no change above 23.4 mrad at 200 kV. The minimum thickness that could be measured using EELS at 300 kV was found to be about 18 nm for a crystalline Si. Additionally, in case of crystalline Si, it is noted that beam direction affect to mean free path under small collection angle.

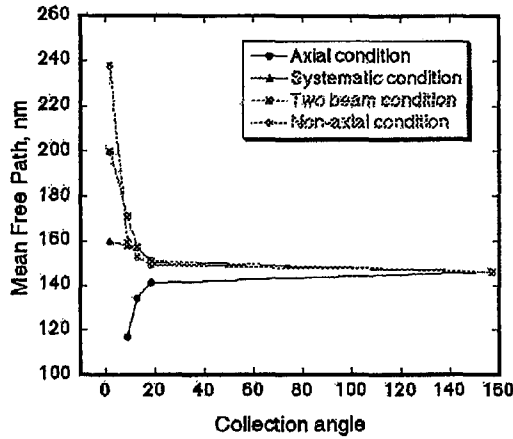


Fig. 5. The effect of beam direction on the mean free path ( $\lambda_p$ ) of crystalline Si.

Figure 5 shows effect of beam direction on  $\lambda_p$ . There is no significant difference of  $\lambda_p$  between axial and non-axial conditions without objective aperture (large collection angle). However, in small collection angle region, the different values of  $\lambda_p$  between axial and non-axial condition become larger. The reason can be explained as follow. Some elastically scattered electrons are present apart from the origin as change from non-axial condition to axial condition, whereas in elastically scattered electrons are still mostly present around the origin. Th en if th e incident beam direction ch anges from axial condition to non-axial condition, the dynamical diffraction effect becomes insignificant, th rough some fraction of th e transmitted beam will ch ange from Bragg reflections concentrate in origin. Th e distribution of inelastically scattered electrons can be also modified by the dynamical diffraction effect, but the modulation will be much smaller than the case of elastic scattering. As a result, the intensity ratio of elastic and inelastic scattering is modified and hence the parameter  $\ln(I/I_0)$  will be increased when a small objective aperture is inserted around the transmitted beam. Therefore, beam direction must be considered at thickness measurement by using EELS in crystalline materials.

The mean inner potential ( $U_0$ ) of a crystalline Si was evaluated to be  $10.8 \pm 0.7$  V by using electron holography. Comparing a calculated value, the experimental data has difference of about 30%, and it is found that the reason of the deviation is due to the dynamical diffraction effect, the accuracy in measuring holograms, and the limitation of non-binding approximation for calculation.

## Chapter 6 Conclusions

(1) The visibility of interference fringes is estimated to be between 0.5 and 0.02 under the condition that biprism voltage has values between 20 – 90V. Under the condition of no objective aperture and current density at  $5.0 \text{ pA/cm}^2$ , amount of charging on  $\text{SiO}_2$  particles are estimated to be  $1.403 \times 10^{-16}$  C and this charge is equal to the net loss of about 880 electrons emitted from  $\text{SiO}_2$  particle since the elementary electric charge is  $1.6 \times 10^{-19}$  C.

(2) From EELS, the mean free path ( $\lambda_p$ ) of an amorphous  $\text{SiO}_2$  and crystalline Si were estimated to be  $178 \pm 4$  nm and  $147 \pm 5$  nm under the condition of no objective aperture at 200 kV. Under no objective aperture condition,  $\lambda_p$  for inelastic scattered electron was found to decrease with the decreasing of accelerating voltage. Indeed,  $\lambda_p$  increases rapidly with the decreasing of collection angles from 2.1 mrad to 23.4 mrad, whereas there is no change above 23.4 mrad at 200 kV.

(3) From electron holography, the mean inner potential ( $U_0$ ) of amorphous  $\text{SiO}_2$  and crystalline Si were evaluated to be  $11.5 \pm 0.3$  V and  $10.8 \pm 0.7$  V, respectively. The accurate thickness measurement in a thinner region is more possible for electron holography than EELS in amorphous  $\text{SiO}_2$ .

## 審査結果の要旨

透過電子顕微鏡法において試料の厚さの精密な測定は、格子欠陥密度の定量的な評価や高分解能電子顕微鏡法による構造解析において重要な因子である。これまで幾つかの厚さ測定法が提唱されてきたが、それぞれ、結晶材料にしか適用出来ない、また測定精度が低いなどの欠点を有していた。本研究では、Si 結晶と非晶質 SiO<sub>2</sub> の平均内部ポテンシャルと電子の非弾性散乱平均自由行程を求めると共に、電子線ホログラフィーと電子エネルギー損失分光法を用いて、高い精度でこれら試料の厚さ評価を行ったものである。

第1章では、本研究の背景として電子顕微鏡法における厚さ測定の重要性と研究目的について述べている。

第2章では、本研究で用いた電子線ホログラフィーと電子エネルギー損失分光法の原理と実験方法について述べている。

第3章では、電子線ホログラフィーの精度を左右する可視度に影響を及ぼす因子を評価すると共に、電子線ホログラフィーに関する最適な実験条件を明らかにしている。さらに、電子線照射によって生じる非晶質 SiO<sub>2</sub> の帯電効果についても定量的な評価を行っている。

第4章では、非晶質 SiO<sub>2</sub> の内部ポテンシャルと電子の非弾性散乱平均自由行程を測定すると共に、電子線ホログラフィーと電子エネルギー損失分光法を用いて種々の実験条件でその厚さ評価を実施している。具体的には、電子線ホログラフィーを用いた場合には、数 nm の薄膜まで厚さを精度よく評価できることを見出している。また電子エネルギー損失分光法を用いた場合には、約 20nm から約 1000nm の厚さ範囲まで比較的高い精度で厚さ評価が可能であることを明らかにしている。さらに電子顕微鏡の加速電圧や散乱電子の取りこみ角の変化に対する、電子の非弾性散乱平均自由行程の変化を測定し、理論的に見積もられる値との比較、検討も行っている。

第5章では、Si 結晶に対する厚さ評価の精度について述べている。特に、Si 結晶については結晶特有の動力的回折効果について検討を行い、電子線ホログラフィーの測定精度に大きな影響を及ぼすことを明らかにしている。さらに電子の非弾性散乱平均自由行程の評価に対する電子の入射方向の影響も検討し、取りこみ角が小さい場合、動力的回折効果が電子エネルギー損失分光法の測定精度を低下させることを明らかにしている。

第6章では、本研究で得られた成果を総括している。

以上要するに、本論文は、電子線ホログラフィーと電子エネルギー損失分光法の最適実験条件を明らかにすると共に、これらの解析法を用いて Si 結晶と非晶質 SiO<sub>2</sub> の精密な厚さ評価を行ったものであり、これらの評価は材料加工プロセス学の発展に寄与するところが少なくない。

よって、本論文は博士（工学）の学位論文として合格と認める。